

Predicting Clinical Course from Subcortical Shape in Provisional Tic Disorder

Authors

Tiffanie Che ¹, Soyoung Kim ², Deanna J. Greene ³, Ashley Heywood ⁴, Jimin Ding ⁵, Bradley L. Schlaggar ⁶, Kevin J. Black ⁷, Lei Wang ^{1,4}

Institutions

¹ Department of Psychiatry and Behavioral Health, Ohio State University Wexner Medical Center, Columbus, OH; tiffanieche2019@u.northwestern.edu; Lei.Wang@osumc.edu

² Departments of Psychiatry and Radiology, Washington University in St. Louis School of Medicine, St. Louis, MO; soyoung@brainkim.com

³ Department of Cognitive Science, University of California San Diego, La Jolla, CA; deannagreene@ucsd.edu

⁴ Department of Psychiatry and Behavioral Sciences, Northwestern University Feinberg School of Medicine, Chicago, IL; ashley.heywood@northwestern.edu

⁵ Department of Mathematics and Statistics; Department of Medicine, Washington University in St. Louis, St. Louis, MO; jmding@wustl.edu

⁶ Kennedy Krieger Institute, Baltimore, MD; Departments of Neurology and Pediatrics, Johns Hopkins University School of Medicine, Baltimore, MD; schlaggar@kennedykrieger.org

⁷ Departments of Psychiatry, Neurology, Radiology and Neuroscience, Washington University in St. Louis School of Medicine, St. Louis, MO; kevin@wustl.edu

Abstract

The ongoing NewTics study examines children who have had tics for less than 9 months (NT group), a population on which little research exists. Here, we further investigate relationships between subcortical shape and tic symptom outcomes. 187 children were assessed at baseline and a 12-month follow-up: 88 with NT, 60 tic-free healthy controls (HC), and 39 with chronic tic disorder or Tourette syndrome (TS), using T1-weighted MRI and total tic scores (TTS) from the Yale Global Tic Severity Scale to evaluate symptom change. Subcortical surface maps were generated using FreeSurfer-initialized large deformation diffeomorphic metric mapping, and linear regression models were constructed to correlate structural shapes with TTS while accounting for co-variates, with relationships mapped onto structure surfaces. We found the NT group to have a larger right hippocampus compared to healthy controls. Subsequent analyses including clinical symptoms revealed a significant correlation between the future worsening of tic symptoms and a larger pallidum and thalamus at baseline. Surface maps illustrate distinct patterns of inward deformation (localized volume loss) in the putamen and outward deformation (localized volume gain) in the thalamus for the NT group compared to healthy controls. We also found distinct patterns of outward deformation in almost all studied structures when comparing the TS group to healthy controls. In the significant vertices of

this comparison, the caudate further exhibited an overall trend of outward deformation compared to the average template in the TS group compared to both the NT group and controls. When comparing the NT and TS groups, the NT group showed consistent outward deformation in the caudate, accumbens, putamen, and thalamus. Since the NT group has had tics only for a few months, we can rule out the possibility that these subcortical volume differences are caused by living with tics for years; they are more likely related to the cause of tics. These observations constitute some of the first prognostic biomarkers for tic disorders and suggest localized circuitry that may be associated with outcome of tic disorders.

Introduction

Chronic tic disorders (CTD) were once thought to be rare but are now known to be relatively common [1]. Tics are sudden, repetitive, nonrhythmic movements or vocalizations such as blinks or grunting [2]. Transient tics affect at least 20% of children, though only about 3% of all children have tics for a full year, the requirement to diagnose a chronic tic disorder or Tourette syndrome (TS) [3, 4]. When tics are present but have not yet persisted for one year since onset, Provisional Tic Disorder is diagnosed [1]. Efforts to identify biomarkers for tics and study the pathophysiology of tic disorders have recently been increasing, although our understanding is still limited [5, 6].

Studies exploring differences in subcortical structure and function have often been contradictory, with some finding no significant differences in basal ganglia volumes or shape between children with TS and matched control children [6]. Two groups found increased putamen volume in TS compared to HC, but a larger study found decreased volume [7-9]. A large study of basal ganglia volume in vivo found the caudate to be 4.9% smaller in the TS group [10]. Smaller studies found lower caudate volume [11, 12], and another large study identified no change [13].

Previous such studies have also primarily focused only on TS (diagnosed chronic tics) and control samples. Therefore, we cannot determine whether the identified differences reflect an underlying cause of tics or secondary changes due to prolonged tic presence. Examining participants at the onset of tic symptoms will more likely lead to identifying biomarkers related to the primary cause of tics.

Thus, the NewTics study examined children who had experienced tics for less than 9 months (median 4 months; new tics, or NT) [14]. Little research exists on this population, and there are even fewer results on predictive outcome analyses, which have also been contradictory [4]. The NewTics study aimed to see whether features including subcortical structures measured shortly after tic onset can predict symptom severity 12 months after tic onset [14]. A previous volumetric MRI analysis using data from 65 children with NT found that striatal volumes did not predict outcome, but a larger hippocampus at baseline predicted worse severity at follow-up [15].

In the present study, we further investigated neurobiological characteristics and predictors of tic disorders by examining relationships of the *shape* of these subcortical structures with tic symptom outcomes (NT) and with diagnosis (NT, TS, and tic-free controls). Three-dimensional surface analysis can detect subtler or more localized volumetric changes that are not revealed in whole-structure, scalar volumetric analysis [16]. Using whole-structure volume estimates alone may yield false negative findings by overlooking local deformities in shape. Previously, diffeomorphic mapping of structural magnetic resonance imaging (MRI) has successfully mapped pathological biomarker patterns onto surface-based representations of anatomical structures [17].

We predicted that baseline volumes would differ across NT, TS, and control groups, and that subcortical shape would demonstrate distinct patterns of shape deformation in tic disorders. We further predicted that we would find distinct regions of shape deformation in subcortical structures at baseline that predict clinical outcome in terms of tic severity changes after one year. We also tested whether shape deformation analyses would confirm the previous finding that hippocampal volume predicted symptom severity outcome, using a 3D method in an expanded sample.

Materials and Methods

Subjects and data collection

Subjects. The sample consisted of 187 children across 3 groups: children examined within 9 months after tic onset (median 3.5 months; new tic, or NT), tic-free children with no parental or sibling history of tics (healthy controls, HC), and children who at the time of screening already have TS/CTD (TS group) [14]. NT subjects returned for clinical evaluation at the one-year anniversary of the best estimate of tic onset. For TS and HC subjects, follow-up visits occurred as near as possible to the same time after screening as it did for their matched NT subject, based on age, sex, and handedness.

Enrollment criteria. Subjects were limited to ages 5-15 at enrollment to reduce sample variance (changed to ages 5-10 after enrolling only 2 participants over age 10 in the first year or so). NT children had current tic symptoms, with the first tic starting less than 9 months before enrollment. Exclusion criteria are detailed elsewhere [14]. The TS group included children who met DSM-5 criteria for TS/CTD at enrollment. The exclusion criteria used reflect those of the NT group. Control children had no current or past tics.

Clinical data collection. For participants exhibiting tic symptoms, a best-estimate date of onset was taken as described in [18]. Total tic scores from the Yale Global Tic Severity Scale (YGTSS), reflecting current tic severity, were determined during a neurological and psychiatric examination performed by Dr. Black for NT and TS subjects. Additional assessments were done at the time of screening [14]. The

YGTSS is a tool used to quantify the severity of tic symptoms in children and adolescents. The Total Tic Severity Score (TTS) comprises half of the YGTSS score and has a range of 0-50; a higher score indicates more severe tic symptoms [19].

Imaging data collection. All subjects at entry were assessed through 1 mm³ T1-weighted magnetization prepared rapid gradient echo (MPRAGE) images and T2-weighted images using three different scanners across the data acquisition period. Details of scan parameters are given in Kim et al (2020) [15]. About half of the scans (the newer ones) were acquired with a prospective motion correction sequence (vNavs) that substantially reduced head motion artifact [20].

Additional measures were taken prior to scanning to reduce motion effects on images, including the use of a mock scanner, as well as an informational video and a game for children to practice holding still during scanning, adapted from a previous study in children [21].

Data processing / Image processing

Data processing began with the use of the FreeSurfer (version 6.0.0) software's probabilistic voxel-based classification, which provided initial subcortical segmentations [22]. Surfaces of the hippocampus, amygdala, basal ganglia (caudate, putamen, pallidum, and nucleus accumbens), and thalamus were automatically generated for each participant using multi-atlas FreeSurfer-initialized large deformation diffeomorphic metric mapping (FS+LDDMM), which utilizes automated brain segmentations based on multiple template images and allows for image alignment and intensity normalization to produce smooth transformations for each region of interest [22, 23]. Combining maps from multiple atlases that best match an individual's scan features has shown improved segmentation accuracy and reduced biases [24]. An experienced rater (the first author) inspected the final surfaces and made minor manual edits on the initial segmentation on poor surface maps, affecting maps of 6 subjects. The edited segmentations were then re-processed via LDDMM to yield accurate maps to be included in subsequent surface analyses.

Surfaces were then scaled with a scale factor calculated for each subject using the population TIV (estimated total intracranial volume) over the individual's TIV, as well as the voxel resolution of their scan. To calculate the (one-dimensional) scale factor, we used the formula: $(\text{Population TIV} / \text{Individual TIV})^{1/3} * \text{Voxel Resolution}$.

Local shape variation for each participant was calculated from the population average of all participants by quantifying the vertex-to-vertex perpendicular change between surfaces, which were assigned a positive (outward variation from the population average) or negative (inward variation from the population average) value [22]. Subcortical volumes for each participant were determined using the volume enclosed within the surfaces. FreeSurfer also reported estimated total intracranial volume (TIV) to be used as a co-

variate in surface analyses, as TIV estimated by FreeSurfer segmentation has been shown to influence subcortical volumes [23].

Statistical analysis

TTS: Paired T-tests were conducted to determine significance of TTS changes from baseline to 12-months within each group, as well as between the NT and TS groups.

TIV: We first conducted a one-way ANOVA on TIV (dependent variable) to determine group (independent variable) effects with post hoc Tukey HSD tests for pairwise differences, with and without age and sex as covariates. The tests showed significant group effects (see results); therefore, TIV was used as an additional covariate in all subsequent analyses.

Scanner type: We first conducted a chi-square test that determined that neither scanner types nor race differed between groups. Additionally, we conducted one-way ANOVA tests to determine the effects of scanner type on structural volumes. We found that the subcortical structures did not differ in volume based on the scanner type, and subsequent ANCOVA and post hoc tests found that group differences found in TIV between NT and healthy controls still occur after controlling for the scanner type. Thus, we did not use scanner as a covariate in subsequent analyses.

Race: The tests done for scanner type (see above) were applied to race as well, and similar results were found. We thus also did not use race as a covariate in subsequent analyses.

Subcortical volumes: Using the surface volumes for each subcortical structure, we first found estimated marginal means and standard errors for each group. ANCOVA and post hoc tests on subcortical volumes (dependent variables) were then conducted to compare group (independent variable) differences of baseline structural volumes, using age and sex as covariates. All structures were examined by combining left and right subcortical structures, since we did not have a lateralized hypothesis. If groups were found to differ significantly for a specific structure, further analyses were conducted to examine left and right structures separately. Analyses done in R used version 4.0.5, with psych and ggplot2 packages [25, 26].

We then performed a partial correlation analysis using baseline structural volume to predict 12-month TTS in the NT group while controlling for screen TTS, age, and sex.

Shape: For group comparisons, ANCOVAs were conducted to compare pairwise group differences of baseline surface shape (i.e., NT vs. HC, TS vs. HC, and TS vs. NT). All models included covariates for age and sex. Surface comparisons were conducted using SurfStat implemented in MATLAB [27]. We applied random field theory (RFT) to identify significant clusters of vertices at the family-wise error rate (FWER) of $p < 0.05$ within each subcortical structure, to account for the multiple comparisons inherent in surface maps [28]. Group differences were visualized as a color map displayed on the overall average surface [22].

We then extracted the significant vertices found in the TS-HC surface comparison in applicable structures and found the mean values of the deformation from the average template of these vertices for each subject. Additionally, significant vertices from the NT-HC surface comparisons were studied to run partial correlation analyses on each subject's mean deformation value and their 12-month clinical score (TTS), while controlling for screen TTS, age, and sex. Subsequently, we repeated this process using significant vertices we extracted from the NT-TS surface comparisons.

Results

Subject demographics and clinical features

In total, we analyzed 187 participants: 60 HC (44M / 16F), 88 NT (63M / 25F), and 39 TS (28M / 11F) (Table 1). Sex, mean age (all near 8 years old), scanner type used, and race did not differ significantly between groups.

Sample Characteristic	HC	NT	TS	Statistics
Total N (M / F)	60 (44M / 16F)	88 (63M / 25F)	39 (28M / 11F)	$\chi^2 = 0.06, p = 0.97$
Mean age (SD) at baseline (years)	8.3 ± 2.0	7.8 ± 1.9	8.4 ± 1.9	$F = 1.83, p = 0.16$
Scanner Type*	15 Trio / 45 Prisma	28 Trio / 60 Prisma	8 Trio / 31 Prisma	$\chi^2 = 1.97, p = 0.37$
Race**	44 White / 10 Black or African American / 5 More than one race / 1 Unknown or not reported	73 White / 6 Black or African American / 6 More than one race / 1 Asian / 2 Unknown or not reported	30 White / 8 More than one race / 1 Asian	$\chi^2 = 17.10, p = 0.07$
Mean TTS at baseline	N/A	$16.96 \pm 5.64; n=80$	N/A	N/A
Mean TTS at 12 months	N/A	$14.16 \pm 6.94; n=80$	N/A	N/A

Table 1. Participant characteristics at baseline or 12-months (as specified under “Sample Characteristic”). Values indicate number or mean \pm SD unless indicated otherwise.

*The scanner type used did not differ between groups ($\chi^2 = 1.97$, $p = 0.16$).

** Race did not differ between groups ($\chi^2 = 17.10$, $p = 0.07$).

Baseline total intracranial volume

The one-way ANOVA on TIV with age and sex as covariates revealed significant group differences [$F(2,182)=3.316$, $p=0.004$; see Fig. 1]. Post hoc Tukey HSD tests revealed that the NT group had smaller TIV than controls at baseline (NT= 1484 ± 154 cm³ and HC= 1596 ± 141 cm³; $p=0.03$). Group differences in TIV between NT and healthy controls remained significant after controlling for both scanner type and race independently. Additionally, the TIV differed significantly across scanner types ($p=0.04$) and race ($p=0.04$). Since TIV differed significantly among groups, we henceforth used baseline TIV as a covariate in subsequent analyses.

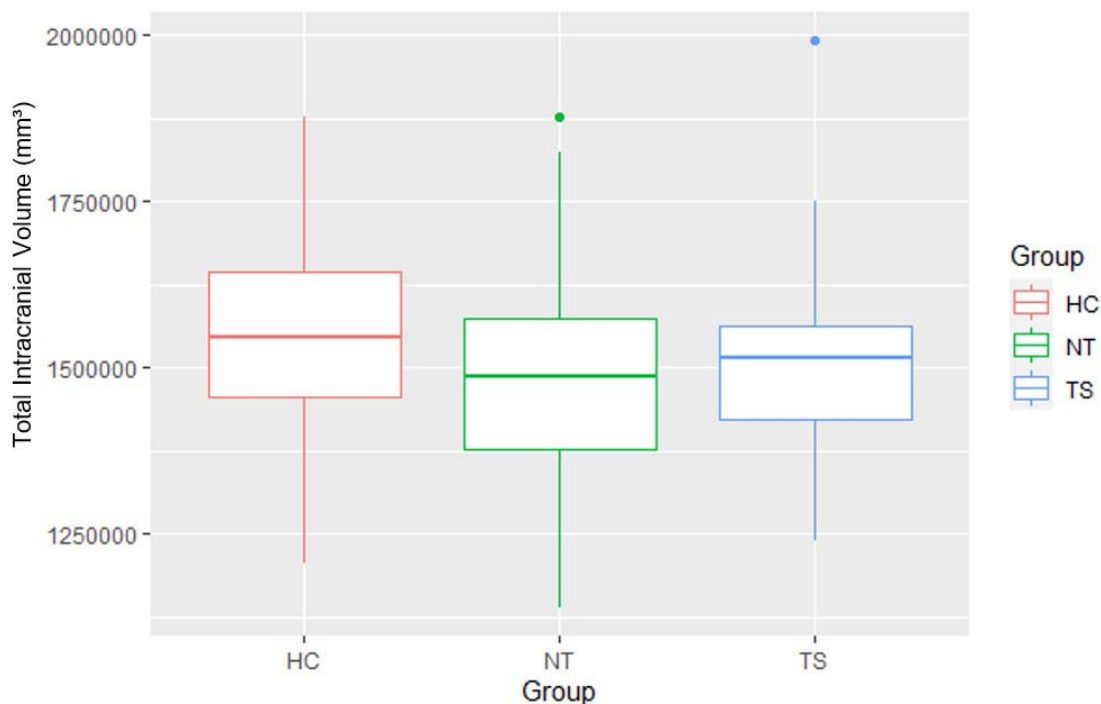


Figure 1. Group comparisons of total intracranial volume measured at baseline. Healthy controls had the highest average, followed by TS and NT. ANCOVA analyses found an overall group effect (see above).

Baseline group comparisons of subcortical structural volumes

Structure	HC	NT	TS	ANCOVA	TukeyHSD
Hippocampus	5394 ± 168	5796 ± 140	5477 ± 205	F(2,182)=2.81, p=0.06	N/A
<i>L Hippocampus</i>	2487 ± 77	2643 ± 64	2507 ± 94	F(2,182)=2.14, p=0.12	N/A
¹ <i>R Hippocampus</i>	2907 ± 92	3153 ± 77	2970 ± 112	F(2,182)=3.38, p=0.04	NT-HC: p=0.04 TS-HC: p=0.88 TS-NT: p=0.23
Amygdala	2782 ± 88	2943 ± 73	2768 ± 107	F(2,182)=2.01, p=0.14	N/A
<i>L Amygdala</i>	1359 ± 43	1425 ± 39	1348 ± 52	F(2,182)=1.51, p=0.22	N/A
<i>R Amygdala</i>	1423 ± 46	1518 ± 38	1420 ± 56	F(2,182)=2.45, p=0.09	N/A
Caudate	7671 ± 274	7700 ± 228	7201 ± 334	F(2,182)=0.83, p=0.44	N/A
<i>L Caudate</i>	3784 ± 134	3796 ± 112	3568 ± 164	F(2,182)=0.72, p=0.49	N/A
<i>R Caudate</i>	3887 ± 140	3904 ± 117	3633 ± 171	F(2,182)=0.94, p=0.39	N/A
Accumbens	877 ± 32	878 ± 27	831 ± 39	F(2,182)=0.50, p=0.61	N/A
<i>L Accumbens</i>	438 ± 16	439 ± 14	418 ± 20	F(2,182)=0.36, p=0.70	N/A
<i>R Accumbens</i>	439 ± 16	439 ± 13	413 ± 19	F(2,182)=0.65, p=0.53	N/A
Putamen	10766 ± 385	10592 ± 321	10308 ± 470	F(2,182)=0.29, p=0.75	N/A
<i>L Putamen</i>	5214 ± 187	5142 ± 156	4986 ± 228	F(2,182)=0.31, p=0.74	N/A
<i>R Putamen</i>	5552 ± 198	5451 ± 165	5322 ± 242	F(2,182)=0.28, p=0.76	N/A
Pallidum	3677 ± 122	3616 ± 102	3624 ± 149	F(2,182)=0.09, p=0.91	N/A
<i>L Pallidum</i>	1836 ± 61	1806 ± 51	1813 ± 75	F(2,182)=0.08, p=0.92	N/A
<i>R Pallidum</i>	1841 ± 61	1810 ± 51	1811 ± 75	F(2,182)=0.10, p=0.91	N/A
Thalamus	14868 ± 521	14438 ± 434	14083 ± 635	F(2,182)=0.50, p=0.61	N/A
<i>L Thalamus</i>	7558 ± 263	7358 ± 219	7165 ± 321	F(2,182)=0.48, p=0.62	N/A
<i>R Thalamus</i>	7310 ± 258	7080 ± 215	6918 ± 315	F(2,182)=0.52, p=0.60	N/A

Table 2. Subcortical Structural Volumes, Accounting for Age and Sex. Significant group differences were found in the hippocampus using a one-way ANCOVA while controlling for age and sex. Post hoc Tukey HSD tests further revealed a specific group difference:

¹ NT had larger right hippocampal volumes than healthy controls ($p = 0.04$).
Values indicate estimated marginal means ± SE unless indicated otherwise.

Table 2 summarizes the estimated marginal means and standard errors of the subcortical volume for each group accounting for age and sex, as well as statistical comparisons for each group. Here, we describe the results for each structure in detail.

Hippocampus. There were no statistically significant differences (though very near significance) among groups when examining the entire hippocampus. However, differences between the NT group and healthy controls were found when isolating the right hippocampus. Patients in NT had on average an 8.5% larger hippocampus compared to those in the HC group.

Amygdala, caudate, accumbens, putamen, pallidum, and thalamus. No group differences were found among HC, NT, and TS groups.

Prediction of 12-month TTS from baseline structural volume

Longitudinal TTS analyses included 80 NT subjects. Over the course of the 12 months between the baseline and second visits, the average TTS decreased significantly from 16.96 ± 5.64 to 14.16 ± 6.94 ($t = 3.82$, $df = 79$, $p\text{-value} = 0.0003$).

Partial Correlation between Baseline Volume and TTS Change (controlled for screen TTS, age, & sex; $n=80$)		
Structure	TTS Change (r)	p-Value
Hippocampus	0.18	0.12
Amygdala	0.17	0.14
Caudate	0.21	0.06
Accumbens	0.15	0.20
Putamen	0.19	0.09
Pallidum	0.24	0.04
Thalamus	0.23	0.05

Table 3. Partial Correlation between Baseline Volume and TTS (controlled for screen TTS, age, & sex; $n=80$).

Table 3 summarizes the partial correlation values between structural baseline volumes and TTS changes, while controlling for screen TTS, age, and sex. Here, we describe the results for each structure in detail.

Hippocampus, amygdala, caudate, accumbens, and putamen. Scaled baseline structural volumes did not predict TTS changes in the NT group.

Pallidum. We found a significant positive correlation between baseline pallidal volume and TTS change from baseline to 12-month measurements ($r=0.24$, $p=0.04$). In other words, a larger pallidum at baseline was significantly correlated with the worsening of tic symptoms.

Thalamus. We found a significant positive correlation between baseline thalamic volume and TTS change from baseline to 12-month measurements ($r=0.23$, $p=0.05$). In other words, a larger thalamus at baseline was significantly correlated with the worsening of tic symptoms.

Baseline group comparisons of subcortical structural shape

When comparing the NT group to healthy controls, two structures were found to have significant regions of deformation as described below.

Putamen. (Figure 2 Panel A). Inferiorly, a small region of inward deformation is seen in the right medial putamen.

Thalamus. (Figure 2 Panel B). We found a region of outward deformation in the medial parts of the left thalamus inferiorly.

Hippocampus, amygdala, caudate, accumbens, and pallidum. No group differences were found among HC, NT, and TS groups.

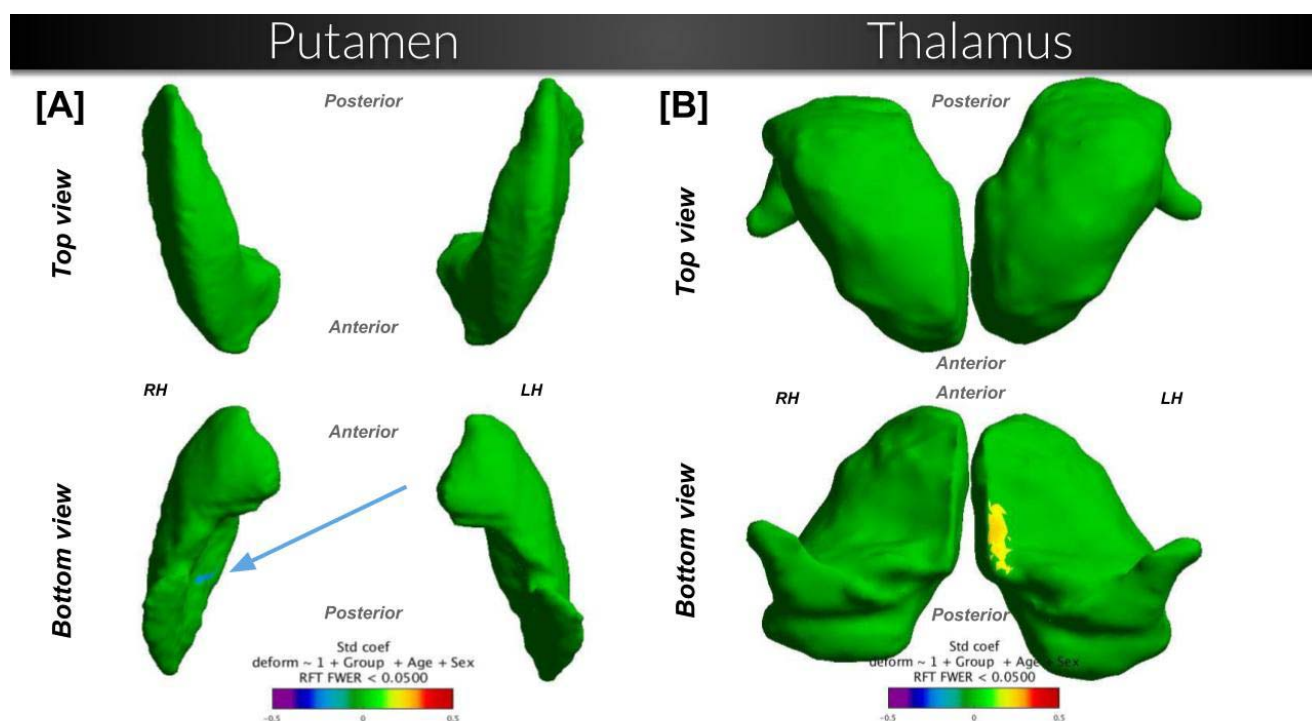


Figure 2. Shape comparison between NewTics vs. Healthy Controls ($n=88$ NT and 60 HC), while controlling for the effects of age and sex. Surfaces are scaled by total intracranial volume and voxel resolution. Cooler shades represent a greater inward deformation of the first group relative to the second, whereas warmer shades represent greater outward deformation. RFT = comparisons that passed the random field theory threshold.

When comparing the NT group to TS children, six structures were found to have significant regions of deformation as described below.

Hippocampus. (Figure 3 Panel A). Superiorly, regions of outward deformation are concentrated towards the lateral-posterior parts of both the left and right hippocampus.

Amygdala. No group differences were found among HC, NT, and TS groups.

Caudate. (Figure 3 Panel B). Superiorly, large regions of outward deformation can be seen along the lateral edge of both the left and right caudate. Inferiorly, regions of outward deformation are seen in the medial anterior parts of the left and right caudate. Additionally, a small region of inward deformation exists along the lateral edge of the left caudate inferiorly.

Accumbens. (Figure 3 Panel C).

Putamen. (Figure 3 Panel D). Inferiorly, a small region of inward deformation is seen in the right medial putamen.

Thalamus. (Figure 3 Panel E). We found a region of outward deformation in the medial parts of the left thalamus inferiorly.

Pallidum. (Figure 3 Panel F). We found regions of outward deformation in both the left and right pallidum inferiorly and superiorly.

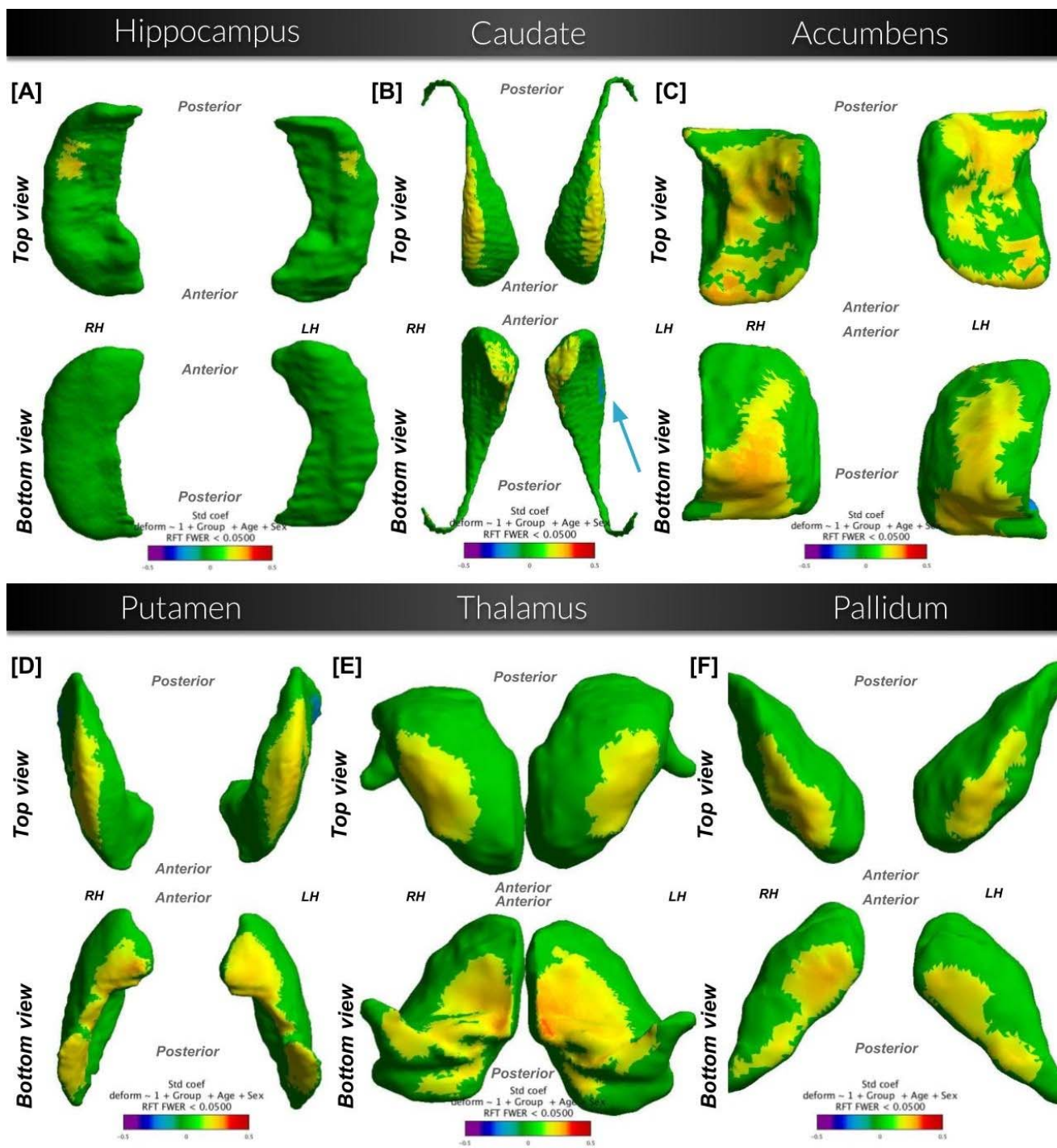


Figure 3. Shape comparison between NewTics vs. Tourette Syndrome (n=88 NT and 39 TS), while controlling for the effects of age and sex. Surfaces are scaled by total intracranial volume and voxel resolution. Cooler shades represent a greater inward deformation of the first group relative to the second, whereas warmer shades represent greater outward deformation. RFT = comparisons that passed the random field theory threshold.

When comparing the TS group to healthy controls, four structures were found to have significant regions of outward deformation. In other words, areas of outward deformation described below illustrate localized volume gain in the specified regions in TS.

Hippocampus, amygdala, and pallidum. No group differences were found among HC, NT, and TS groups.

Caudate. (Figure 3 Panel A). Inferiorly, two small regions of outward deformation is seen in the both the left and right medial caudate.

Accumbens. (Figure 3 Panel B). Superiorly and inferiorly, regions of outward deformation can be seen in the right accumbens.

Putamen. (Figure 3 Panel C). Inferiorly, small regions of outward deformation is seen in the left and right medial anterior putamen.

Thalamus. (Figure 3 Panel D). We found regions of outward deformation towards the medial ends of the left and right thalamus.

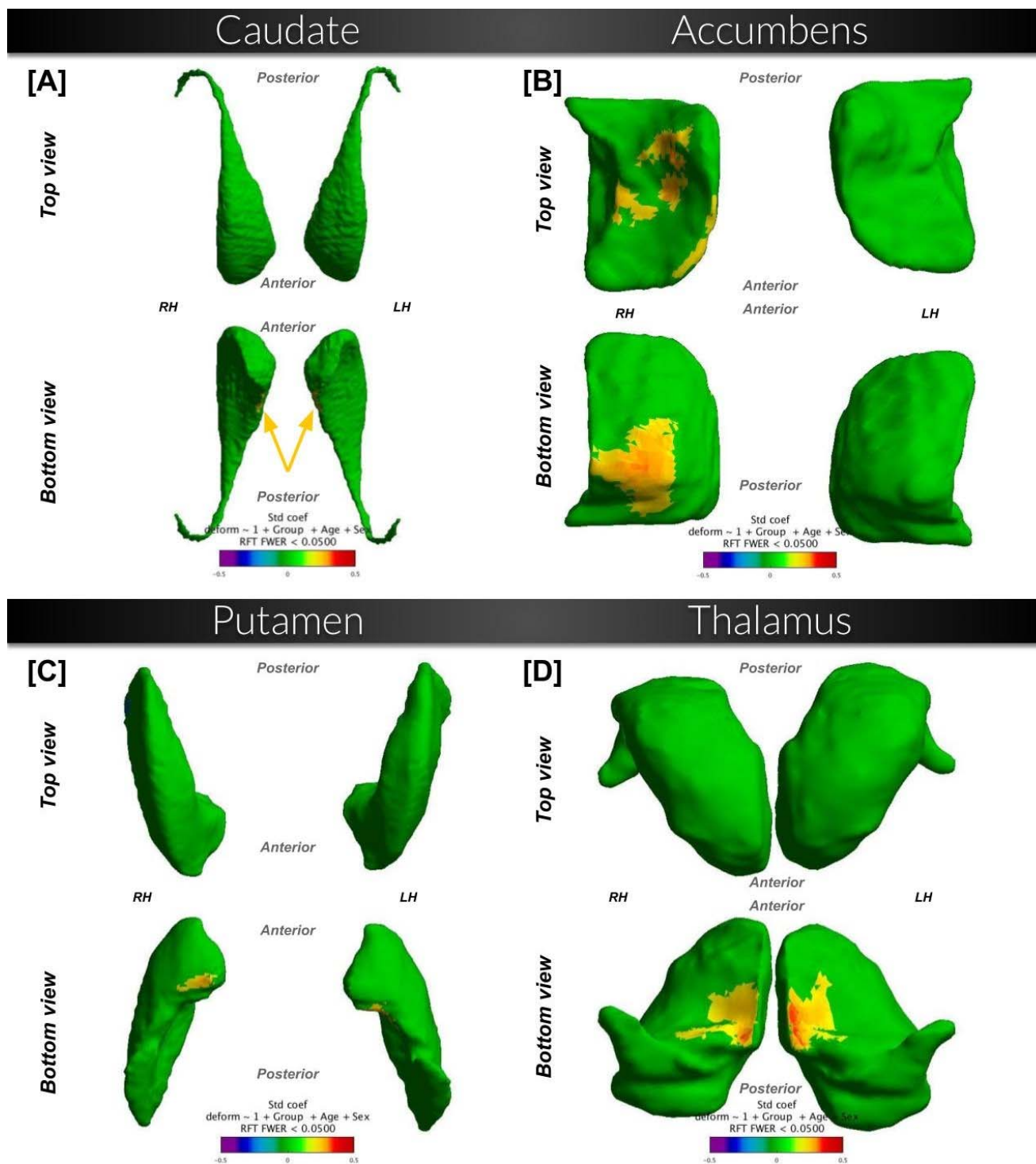


Figure 4. Shape comparison between Tourette Syndrome vs. Healthy Controls ($n=39$ TS and 60 HC), while controlling for the effects of age and sex. Surfaces are scaled by total intracranial volume and voxel resolution. Cooler shades represent a greater inward deformation of the first group relative to the second, whereas warmer shades represent greater outward deformation. RFT = comparisons that passed the random field theory threshold.

Deformation from Average Template Group Values					
<i>n=187</i>					
Structure	HC	NT	TS	ANCOVA	TukeyHSD
Caudate	-0.0489	-0.0510	0.1903	F(2,182)=4.39, p=0.01	¹ TS-HC: p=0.03 ² TS-NT: p=0.02
Accumbens	-0.0611	0.0066	0.0792	F(2,182)=1.91, p=0.15	N/A
Putamen	-0.0222	-0.0158	0.0698	F(2,182)=0.82, p=0.44	N/A
Thalamus	-0.0350	-0.0039	0.0627	F(2,182)=0.45, p=0.64	N/A
All significant vertices	-0.0465	-0.0116	0.0977	F(2,182)=1.85, p=0.16	N/A

Table 4. Deformation from Average Template Group Values. Significant group differences were found in the caudate using a one-way ANCOVA while controlling for age and sex. Post hoc Tukey HSD tests further revealed a specific group difference:

¹ TS demonstrated overall outward deformation from the average template in significant vertices compared to the overall inward deformation seen in healthy controls ($p = 0.03$).

² TS also demonstrated overall outward deformation from the average template in significant vertices compared to the overall inward deformation seen in NT ($p = 0.02$).

Values indicate mean deformation value unless indicated otherwise.

Table 4 summarizes the mean values of the deformation from the average template for each group within the significant vertices found in the TS-HC surface comparison, as well as statistical comparisons for each group. Here, we describe the results for each structure in detail.

Caudate. We found an overall trend of outward deformation compared to the average template in the TS group compared to both the HC and NT groups.

Accumbens. There were no statistically significant differences between groups.

Putamen. There were no statistically significant differences between groups.

Thalamus. There were no statistically significant differences between groups.

All significant vertices. There were no statistically significant differences between groups.

Prediction of 12-month TTS from baseline structural shape

When comparing the NT group with healthy controls, we found that 18 out of the 13638 vertices on the putamen surface had a significant deformation value. On the thalamus, 45 out of 9580 vertices were significant.

NT-HC Partial Correlations between Deformation and 12-month TTS
(controlled for screen TTS, age, and sex; n=80)

Structure	12-month TTS (r)	p-Value
Putamen	0.020	0.863
Thalamus	0.109	0.337
All significant vertices	0.119	0.300

Table 5. NT-HC Partial Correlations between Deformation and 12-month TTS (controlled for screen TTS, age, and sex; n=80).

Table 5 summarizes the correlation and p-values between each NT subject's mean deformation value in the significant vertices of the NT-HC comparison and their 12-month TTS, while controlling for screen TTS, age, and sex. We did not find a significant correlation between mean deformation values and 12-month TTS.

When comparing the NT group with the TS group, amounts of significant vertices on structure surfaces were found as follows: 183/13222 significant vertices on the hippocampus surface; 3734/24744 significant vertices on the caudate surface; 2279/5804 significant vertices on the nucleus accumbens surface; 1030/5398 significant vertices on the pallidum surface; 3345/13638 significant vertices on the putamen surface; 1956/9580 significant vertices on the thalamus surface.

NT-TS Partial Correlations between Deformation and 12-month TTS
(controlled for screen TTS, age, and sex; n=80)

Structure	12-month TTS (r)	p-Value
Hippocampus	-0.101	0.374
Caudate	-0.125	0.274
Accumbens	-0.092	0.421
Pallidum	-0.135	0.235
Putamen	-0.145	0.204
Thalamus	-0.144	0.206
All significant vertices	-0.133	0.242

Table 6. NT-TS Partial Correlations between Deformation and 12-month TTS (controlled for screen TTS, age, and sex; $n=80$).

Table 6 summarizes the correlation and p-values between each NT subject's mean deformation value in the significant vertices of the NT-TS comparison and their 12-month TTS, while controlling for screen TTS, age, and sex. We did not find a significant correlation between mean deformation values and 12-month TTS.

Discussion

In this study, we focus on the first year of tic development (NT group) and identified several baseline subcortical volume and shape characteristics related to tic symptoms, including some that predict clinical tic outcome 3 to 12 (mean 7.9) months later.

Baseline volume analyses showed that the right hippocampus was on average 8.5% larger in NT children compared to healthy controls. We also found a significant correlation between the worsening of tic symptoms and both a larger pallidum and thalamus at baseline.

Surface analyses demonstrated distinct patterns of subcortical surface deformation in several structures across all group comparisons. When comparing the NT group to healthy controls, we found that the putamen exhibited inward deformation (i.e., localized volume loss), while the thalamus showed outward deformation (localized volume gain). Upon comparing the TS group to healthy controls, we found that structures consistently showed patterns of outward deformation in the TS group, found significantly in almost all of the studied structures, including the hippocampus, caudate, accumbens, putamen, thalamus, and pallidum. Similarly, we also found that this pattern was present when comparing the NT group to the TS group, with the NT group showing consistent patterns of outward deformation in the caudate, accumbens, putamen, and thalamus.

In the significant vertices found in the TS-HC surface comparison of the caudate, we found an overall trend of outward deformation compared to the average template in the TS group compared to both the HC and NT groups. When examining the relationship between each NT subject's mean deformation value and their 12-month TTS, we did not find a significant correlation in neither the NT-HC significant vertices nor the NT-TS significant vertices.

Functional implications

Hippocampus. Children in the NT group had larger right hippocampal volume compared to healthy controls. Further, the NT group also exhibited localized volume increases compared to the TS group. The hippocampus plays a role in memory consolidation in both the cognitive and motor domains [29]. Specifically,

the hippocampus supports visuospatial ability and memory. In a study on patients with amnesic mild cognitive impairment, a larger right hippocampus was significantly associated with higher visuospatial memory scores on the Rey's complex figure test, which measures visuospatial ability and memory [30]. Furthermore, in a study on the effects of traumatic brain injury in the hippocampus, damage to the right hippocampus correlated with lower memory scores on the Rey's complex figure test [31]. Our conjecture is that damage here impairs visuospatial ability and memory, and abnormal enlargement may conversely lead to abnormal preservation of visuospatial memory. There is evidence that in children with TS, those with more persistent motor memory show more severe tics, as they were found to take longer to unlearn a previously learned motor pattern [32]. As we saw that the NT group had a larger right hippocampus at baseline compared to healthy controls, perhaps this region may be implicated in tic development and/or persistence.

Basal Ganglia (accumbens, pallidum, putamen, and caudate). Through structural volume analyses, we saw that the worsening of tic symptoms was associated with a larger baseline pallidum. When analyzing shape differences, we found significant patterns of localized volume increases in NT children compared to TS children in all four structures. However, the putamen in the NT group exhibited localized volume loss when compared to healthy controls, but this deformation was concentrated towards the posterior end. Additionally, the TS group exhibited localized volume increases in the caudate, accumbens, and putamen when compared to healthy controls. In the significant vertices found in the TS-HC surface comparison of the caudate, we found an overall trend of outward deformation compared to the average template in the TS group compared to both the HC and NT groups.

The basal ganglia are subcortical nuclei that, along with their associated connections, have been a large focus of TS/CTD research. They are involved in motor control in other movement disorders such as Parkinson's and Huntington's disease. Cortico-striatal-thalamo-cortical (CSTC) circuits are involved in inhibitory control and habit formation, both to which are affected in TS [33, 34]. This understanding may relate to the shape and volume differences we found in basal ganglia structures and the pallidum's association with observed changes in tic symptoms.

Thalamus. In the thalamus, there were no significant volumetric differences between groups. When analyzing surfaces, however, we found that the thalamus displayed localized volume increases in NT children when compared to both TS children and healthy controls. Previous volume and surface morphology studies have found greater grey matter volume and outward deformation in the thalamus of TS children compared to healthy controls, which is again seen here in our surface comparison between TS and healthy children [13, 35]. Further, we found a

significant correlation between a larger thalamus at baseline and the worsening of tic symptoms. The position of the thalamus in CSTC circuits, mediating output from motor-related basal ganglia and motor areas of the cerebral cortex, supports its involvement in motor control [36]. Perhaps this region may be implicated in tic development and/or persistence.

We found the NT group to have a larger right hippocampus at baseline compared to healthy controls. In a prior analysis of a smaller subset of the present sample using different methods, a larger hippocampus at baseline predicted worse severity at follow-up [15]. Since the NT group has had tics for only a few months, the subcortical volume differences in this group are especially meaningful as they are more likely to be related to the cause of tics rather than a result of living with chronic tics.

Our results are also consistent with the results of a meta-analysis on task-based fMRI studies in patients with TS [37]. In the thalamus, the meta-analysis showed a clear overlap of all the conditions involving various aspects of voluntary motor execution, response inhibition, and tic generation. The pallidum and thalamus both showed more consistent activation in free-to-tic conditions. This result is consistent with our findings of larger thalamic and pallidal volume at baseline predicting the worsening of tic symptoms. The meta-analysis also identified a positive correlation between tic severity and BOLD activity in the thalamus and putamen [37]. Similarly, in the putamen and thalamus, we found that the NT group exhibited localized volume gain compared to the TS group, and the TS group showed localized volume gain compared to the healthy controls. It seems that these regions are implicated in both tic severity and persistence.

The primary limitation of this project is the cross-sectional nature of the results, as we are collecting more 12-month scan and TTS data. Future studies shall include longitudinal and within-subject analyses using both baseline and 12-month scans, in combination with clinical scores. Nevertheless, our study is, to our knowledge, the first imaging study of Provisional Tic Disorder.

These new findings have potential clinical relevance, and continuing to investigate neuroanatomical characteristics in TS/CTD may further provide insight into prognostic biomarkers. In many children with Provisional Tic Disorder, tics improve within the first year, often to the point of clinical insignificance. Understanding the mechanisms related to these outcomes may provide clinical insight into the pathophysiological traits in tic disorders and thus potentially lead to improved treatment approaches. In a previous memory study, multiple-session stimulation increased functional connectivity among cortical-hippocampal network regions and simultaneously improved associative memory performance [38]. With a deeper understanding of neural networks related to tic symptoms, we may be able to similarly provide targets that could be manipulated to prevent worsening of tic symptoms.

Author Contributions

Conceptualization, K.J.B., B.L.S. and L.W.; methodology, L.W.; formal analysis, T.C., L.W., J.D.; investigation, K.J.B., D.J.G., B.L.S., and S.K.; data curation, K.J.B. and S.K.; writing—original draft preparation, T.C.; writing—review and editing, all authors; visualization, T.C.; project administration, K.J.B.; funding acquisition, K.J.B., D.J.G. and B.L.S. All authors have read and agreed to the published version of the manuscript.

Funding

Research reported in this publication was supported by the National Institutes of Health: National Institute of Mental Health under award number K24MH087913 to K.J.B.; K01MH104592 to D.J.G.; R01MH104030 to K.J.B. and B.L.S.; R01MH118217 to D.J.G.; National Institute of Neurological Disorders and Stroke R21NS091635 to B.L.S. and K.J.B.; the Washington University Institute of Clinical and Translational Sciences grants UL1RR024992 and UL1TR000448; the Eunice Kennedy Shriver National Institute of Child Health and Human Development of the National Institutes of Health under Award Number U54HD087011 to the Intellectual and Developmental Disabilities Research Center at Washington University, and K23DC006638 to J.E.C. Lieu; the Mallinckrodt Institute of Radiology MIR-IDDRC Pilot Study Fund; the McDonnell Center for Systems Neuroscience; the National Institute of Biomedical Imaging and Bioengineering grant R01 EB020062 to L.W.; the National Science Foundation grants 1734853 and 1636893 to L.W. The studies presented in this work were carried out in part in the East Building MR Facility of the Washington University Medical Center. The content is solely the responsibility of the authors and does not necessarily represent the official views of the National Institutes of Health or of the MIR.

Institutional Review Board Statement

Protocols 201109157 and 201707059 were approved by the Washington University Human Research Protection Office (IRB).

Informed Consent Statement

Each child assented, and a parent (guardian) gave informed consent. Data shared from other projects were shared after appropriate human subjects review and consent.

Data Availability Statement

All data from this project is being archived at the NIMH Data Archive (<https://nda.nih.gov>, study ID C2692).

Conflicts of Interest

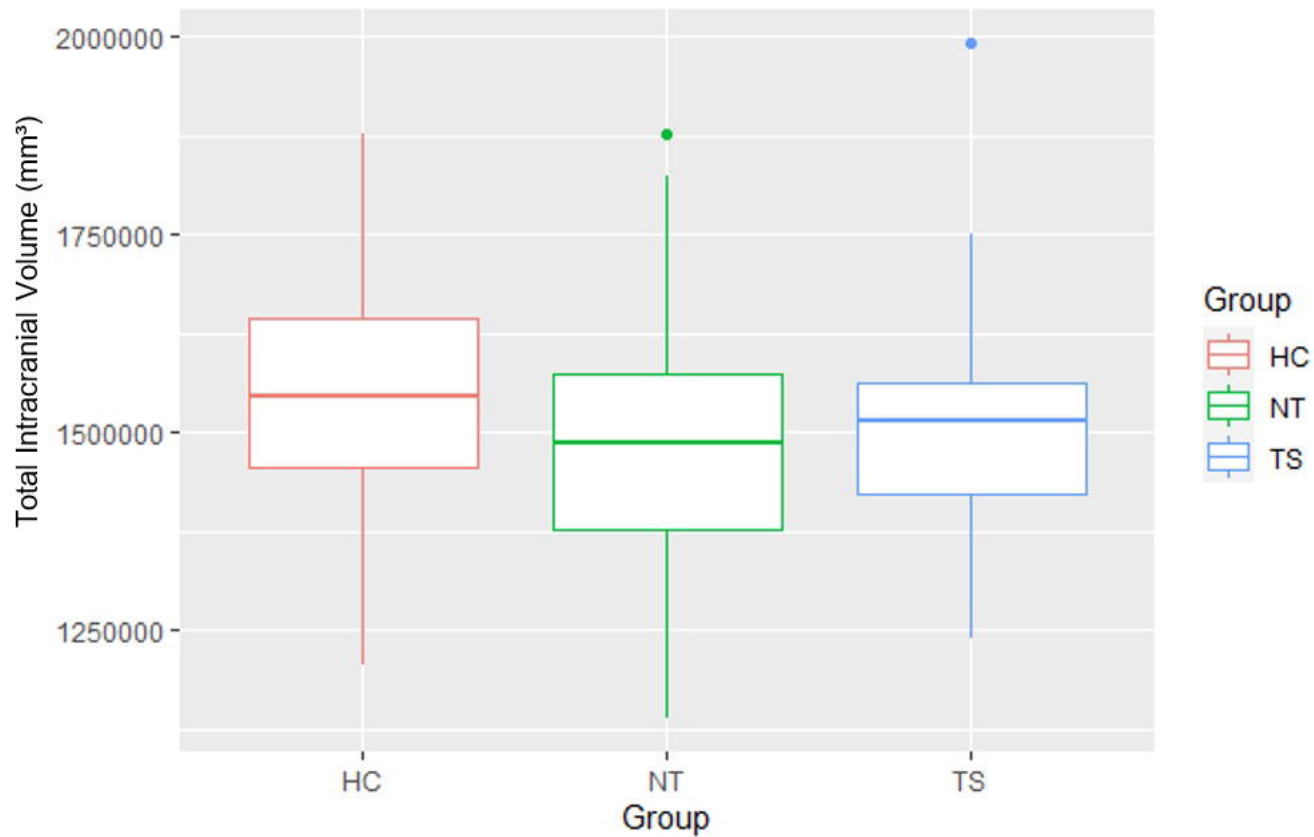
The authors declare no conflict of interest.

References

1. American Psychiatric Association, *Diagnostic and statistical manual of mental disorders, Fifth Edition*. Arlington, VA, American Psychiatric Association. DOI: 10.1176/appi.books.9780890425596. 2013.
2. Black, K.J., *Tics*, in *Encyclopedia of Movement Disorders*. 2010, Chapter 385 (vol. 3, pp. 231-236) in Kompoliti K, Verhagen Metman L (eds.), Oxford: Elsevier (Academic Press), 2010. DOI: 10.1016/B978-0-12-374105-9.00385-3.
3. Scahill, L., M. Specht, and C. Page, *The prevalence of tic disorders and clinical characteristics in children*. *Journal of obsessive-compulsive and related disorders*, 2014. **3**(4): p. 394-400.
4. Black, K.J., et al., *Provisional Tic Disorder: What to tell parents when their child first starts ticcing*. F1000Research, 2016. **5**.
5. Leckman, J.F., et al., *Neurobiological substrates of Tourette's disorder*. *Journal of child and adolescent psychopharmacology*, 2010. **20**(4): p. 237-247.
6. Greene, D.J., K.J. Black, and B.L. Schlaggar, *Neurobiology and functional anatomy of tic disorders*. 2013: Chapter 12 (pp. 238-275) in Martino D, Leckman JF (eds.), *Tourette Syndrome*. Oxford: Oxford University Press, 2013. DOI: 10.1093/med/9780199796267.003.0012.
7. Williams, A.C., et al., *A pilot study of basal ganglia and thalamus structure by high dimensional mapping in children with Tourette syndrome*. F1000Research, 2013. **2**.
8. Ludolph, A.G., et al., *Grey-matter abnormalities in boys with Tourette syndrome: magnetic resonance imaging study using optimised voxel-based morphometry*. *The British Journal of Psychiatry*, 2006. **188**(5): p. 484-485.
9. Roessner, V., et al., *Increased putamen and callosal motor subregion in treatment-naïve boys with Tourette syndrome indicates changes in the bihemispheric motor network*. *Journal of Child Psychology and Psychiatry*, 2011. **52**(3): p. 306-314.
10. Peterson, B.S., et al., *Basal ganglia volumes in patients with Gilles de la Tourette syndrome*. *Archives of general psychiatry*, 2003. **60**(4): p. 415-424.
11. Peterson, B., et al., *Reduced basal ganglia volumes in Tourette's syndrome using three-dimensional reconstruction techniques from magnetic resonance images*. *Neurology*, 1993. **43**(5): p. 941-941.
12. Makki, M.I., et al., *Altered fronto-striato-thalamic connectivity in children with Tourette syndrome assessed with diffusion tensor MRI and probabilistic fiber tracking*. *Journal of Child Neurology*, 2009. **24**(6): p. 669-678.
13. Greene, D.J., et al., *Brain structure in pediatric Tourette syndrome*. *Molecular psychiatry*, 2017. **22**(7): p. 972-980.
14. Black, K.J., et al., *The New Tics study: A novel approach to pathophysiology and cause of tic disorders*. *Journal of psychiatry and brain science*, 2020. **5**.
15. Kim, S., et al., *Hippocampal volume in Provisional Tic Disorder predicts tic severity at 12-month follow-up*. *Journal of clinical medicine*, 2020. **9**(6): p. 1715.
16. Brain Development Cooperative Group, *Total and regional brain volumes in a population-based normative sample from 4 to 18 years: the NIH MRI Study of Normal Brain Development*. *Cerebral Cortex*, 2012. **22**(1): p. 1-12.

17. Wang, L., et al., *Large deformation diffeomorphism and momentum based hippocampal shape discrimination in dementia of the Alzheimer type*. IEEE transactions on medical imaging, 2007. **26**(4): p. 462-470.
18. Greene, D.J., et al., *Reward enhances tic suppression in children within months of tic disorder onset*. Developmental Cognitive Neuroscience, 2015. **11**: p. 65-74. DOI: 10.1016/j.dcn.2014.08.005.
19. Leckman, J.F., et al., *The Yale Global Tic Severity Scale: initial testing of a clinician-rated scale of tic severity*. Journal of the American Academy of Child & Adolescent Psychiatry, 1989. **28**(4): p. 566-573.
20. Tisdall, M.D., et al., *Volumetric navigators for prospective motion correction and selective reacquisition in neuroanatomical MRI*. Magnetic resonance in medicine, 2012. **68**(2): p. 389-399.
21. Barnea-Goraly, N., et al., *High success rates of sedation-free brain MRI scanning in young children using simple subject preparation protocols with and without a commercial mock scanner—the Diabetes Research in Children Network (DirecNet) experience*. Pediatric radiology, 2014. **44**(2): p. 181-186.
22. Jenkins, L.M., et al., *Subcortical structural variations associated with low socioeconomic status in adolescents*. Human brain mapping, 2020. **41**(1): p. 162-171.
23. Wang, L., et al., *Fully-automated, multi-stage hippocampus mapping in very mild Alzheimer disease*. Hippocampus, 2009. **19**(6): p. 541-548.
24. Christensen, A., et al., *Hippocampal subfield surface deformity in nonsemantic primary progressive aphasia*. Alzheimer's & Dementia: Diagnosis, Assessment & Disease Monitoring, 2015. **1**(1): p. 14-23.
25. Revelle, W., *psych: Procedures for Psychological, Psychometric, and Personality Research*. Northwestern University, Evanston, Illinois. R package version 2.1.9, <https://CRAN.R-project.org/package=psych>, 2021.
26. Wickham, H., *ggplot2: Elegant Graphics for Data Analysis*. 1 ed. Use R. 2009: Springer, New York, NY. DOI: 10.1007/978-0-387-98141-3.
27. Worsley, K., et al., *SurfStat: A Matlab toolbox for the statistical analysis of univariate and multivariate surface and volumetric data using linear mixed effects models and random field theory*. Human Brain Mapping, 2009.
28. Taylor, J.E. and K.J. Worsley, *Detecting sparse signals in random fields, with an application to brain mapping*. Journal of the American Statistical Association, 2007. **102**(479): p. 913-928.
29. Schapiro, A.C., et al., *The hippocampus is necessary for the consolidation of a task that does not require the hippocampus for initial learning*. Hippocampus, 2019. **29**(11): p. 1091-1100.
30. Peter, J., et al., *Real-world navigation in amnesic mild cognitive impairment: the relation to visuospatial memory and volume of hippocampal subregions*. Neuropsychologia, 2018. **109**: p. 86-94.
31. Ariza, M., et al., *Hippocampal head atrophy after traumatic brain injury*. Neuropsychologia, 2006. **44**(10): p. 1956-1961.
32. Kim, S., et al., *Visuomotor learning and unlearning in children and adolescents with Tourette syndrome*. Cortex, 2018. **109**: p. 50-59.

33. Aron, A.R., *The neural basis of inhibition in cognitive control*. The neuroscientist, 2007. **13**(3): p. 214-228.
34. Graybiel, A.M., *Habits, rituals, and the evaluative brain*. Annu. Rev. Neurosci., 2008. **31**: p. 359-387.
35. Miller, A.M., et al., *Enlargement of thalamic nuclei in Tourette syndrome*. Archives of general psychiatry, 2010. **67**(9): p. 955-964.
36. Bosch-Bouju, C., B.I. Hyland, and L.C. Parr-Brownlie, *Motor thalamus integration of cortical, cerebellar and basal ganglia information: implications for normal and parkinsonian conditions*. Frontiers in computational neuroscience, 2013. **7**: p. 163.
37. Zapparoli, L., M. Porta, and E. Paulesu, *The anarchic brain in action: the contribution of task-based fMRI studies to the understanding of Gilles de la Tourette syndrome*. Current opinion in neurology, 2015. **28**(6): p. 604-611.
38. Wang, J.X., et al., *Targeted enhancement of cortical-hippocampal brain networks and associative memory*. Science, 2014. **345**(6200): p. 1054-1057.

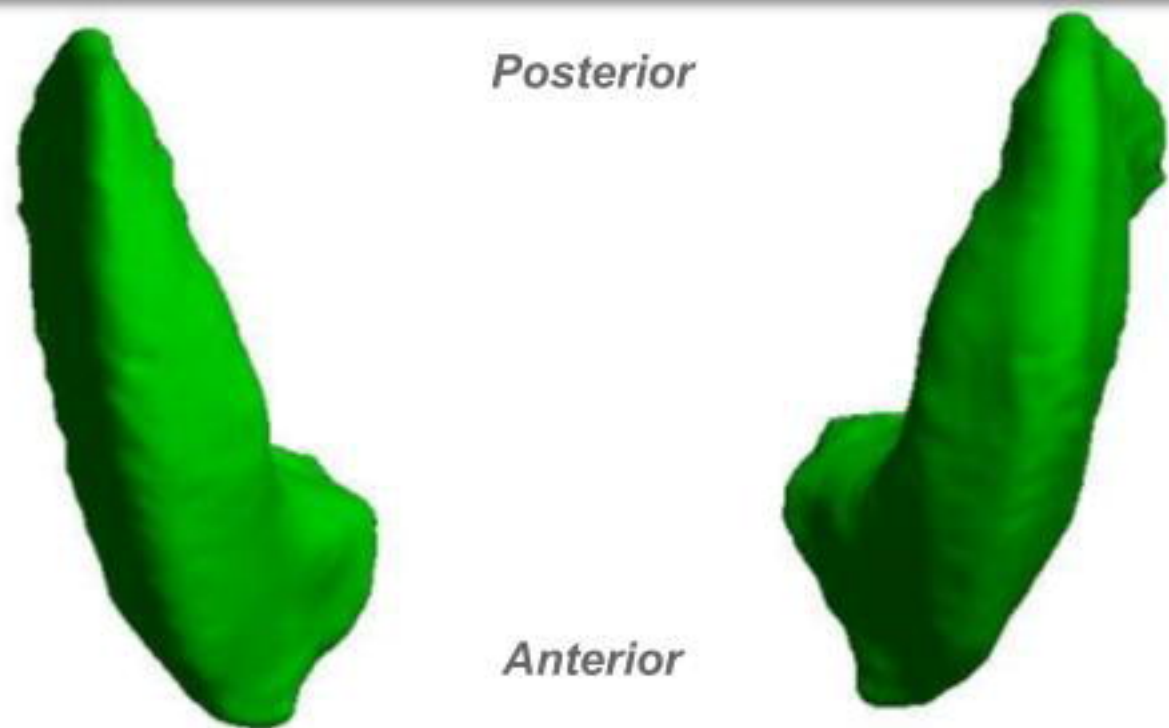


Putamen

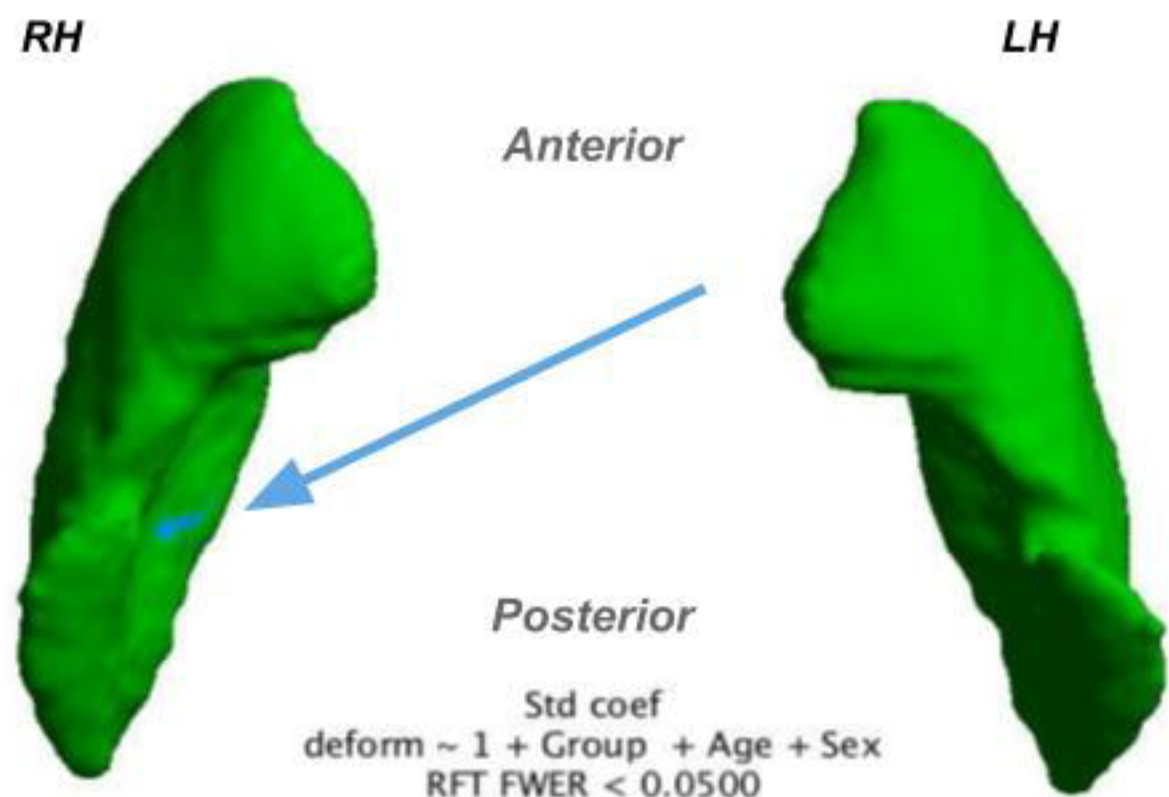
Thalamus

[A]

Top view



Bottom view

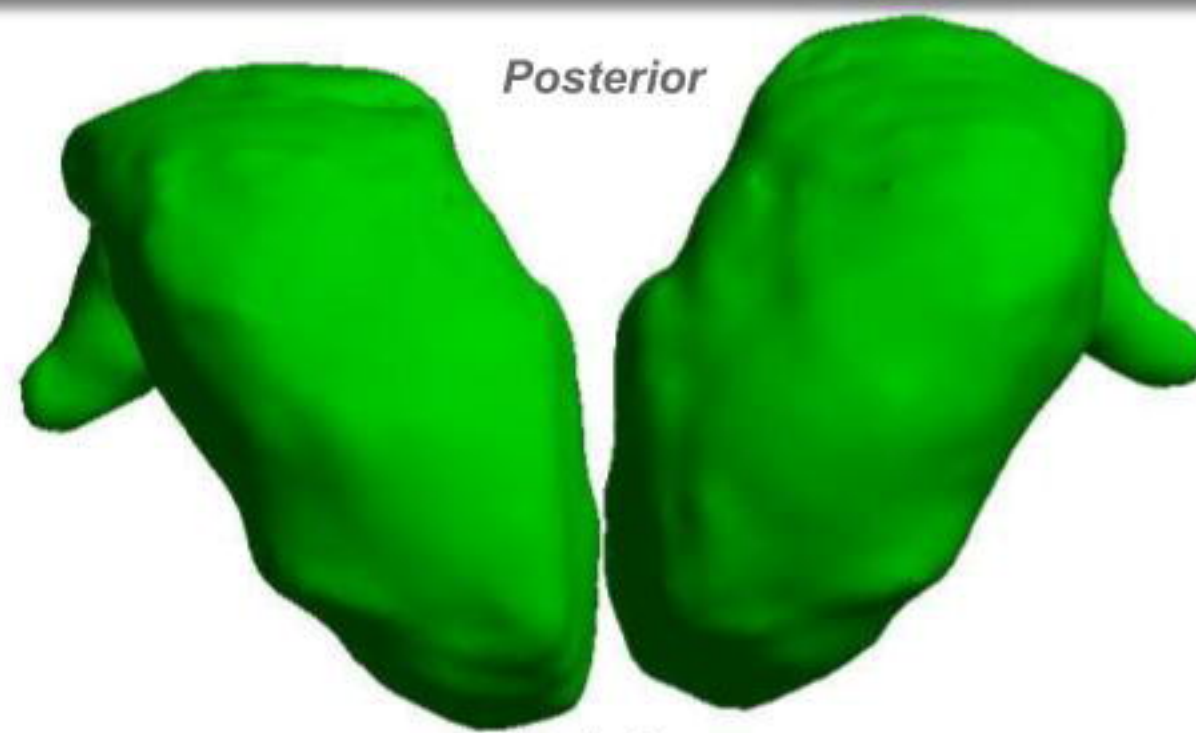


Std coef
deform $\sim 1 + \text{Group} + \text{Age} + \text{Sex}$
RFT FWER < 0.0500

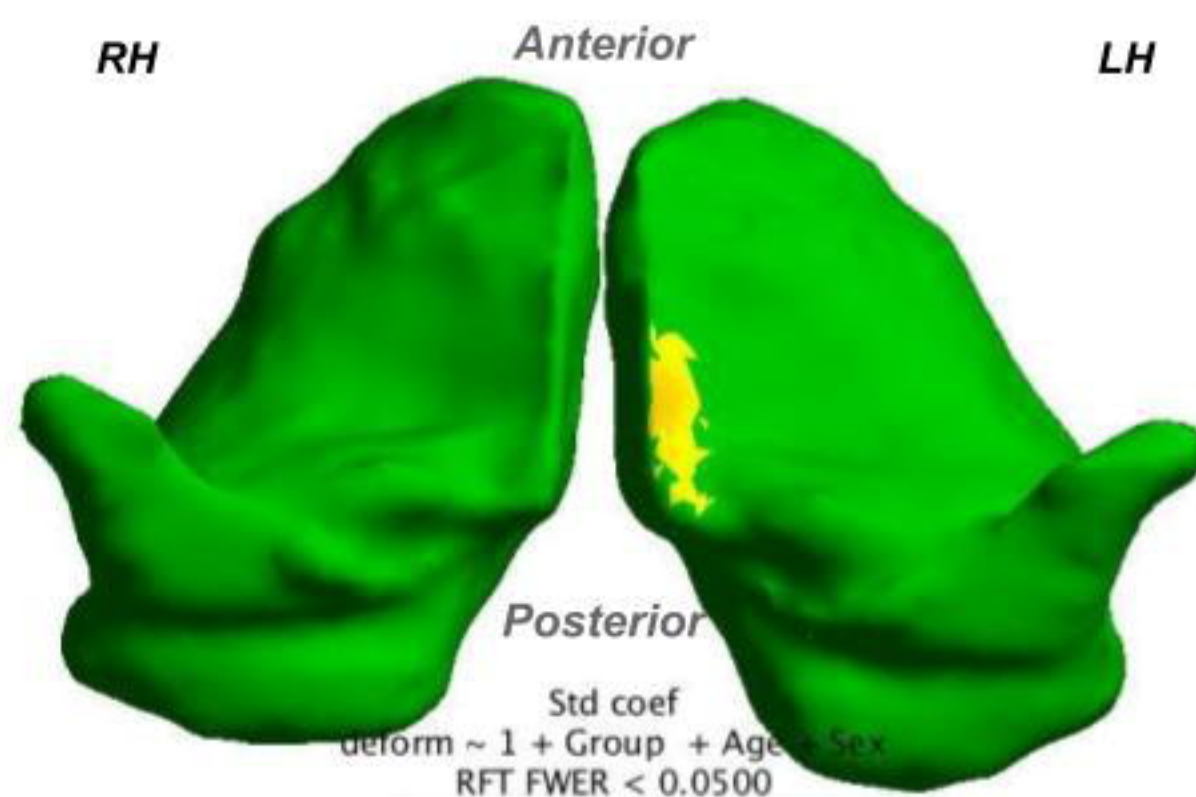


[B]

Top view



Bottom view



Std coef
deform $\sim 1 + \text{Group} + \text{Age} + \text{Sex}$
RFT FWER < 0.0500

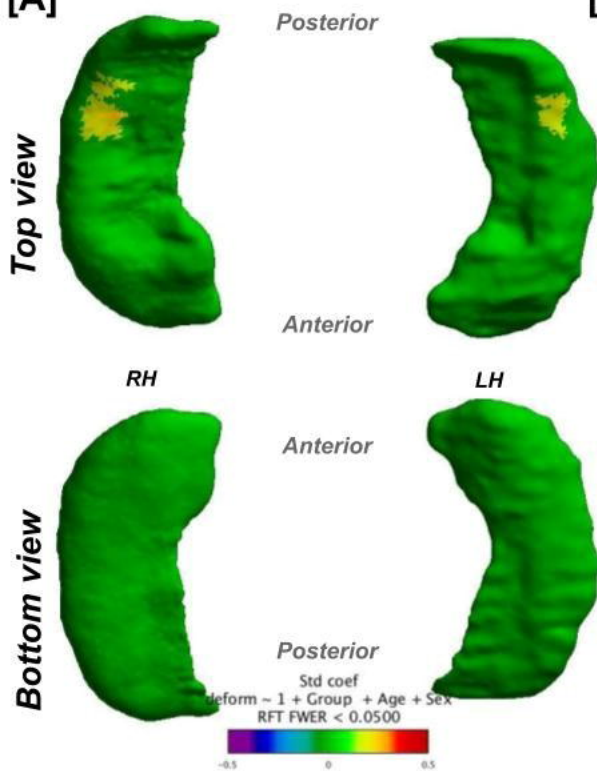


Hippocampus

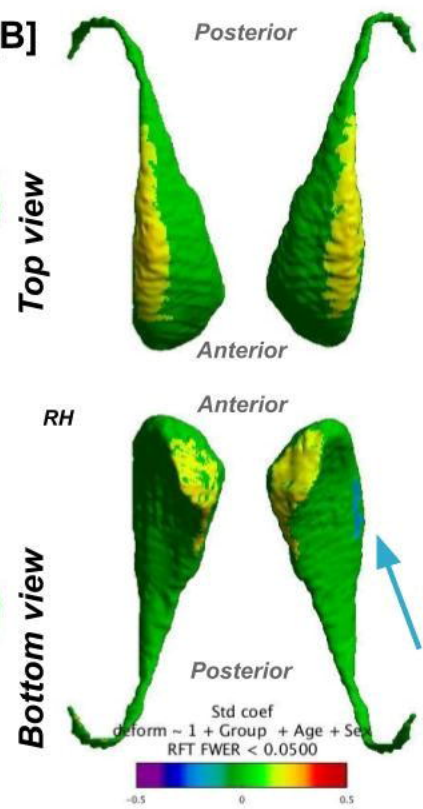
Caudate

Accumbens

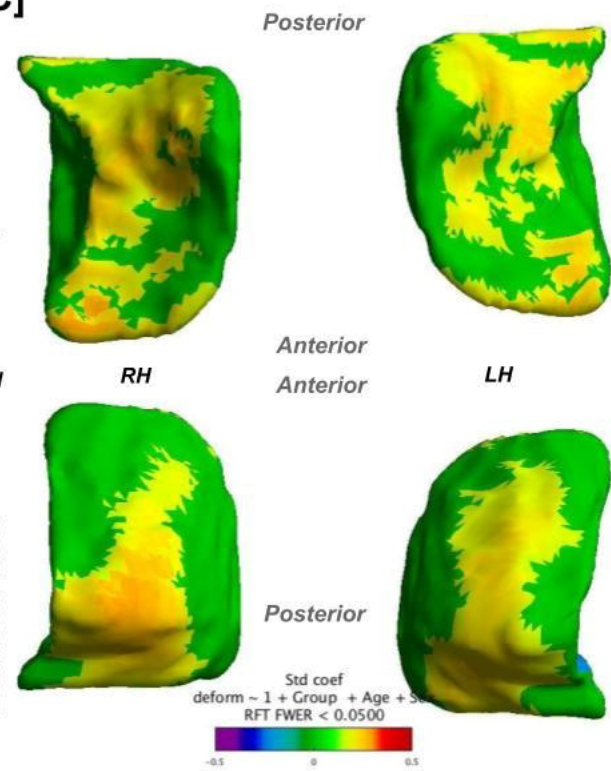
[A]



[B]



[C]

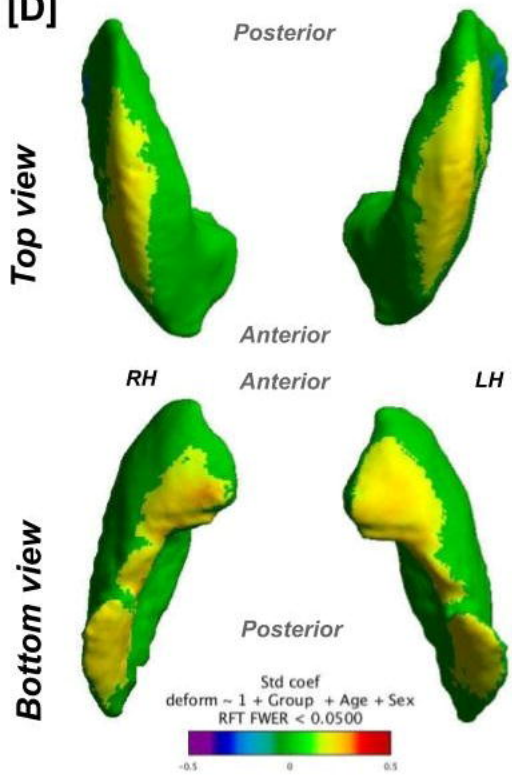


Putamen

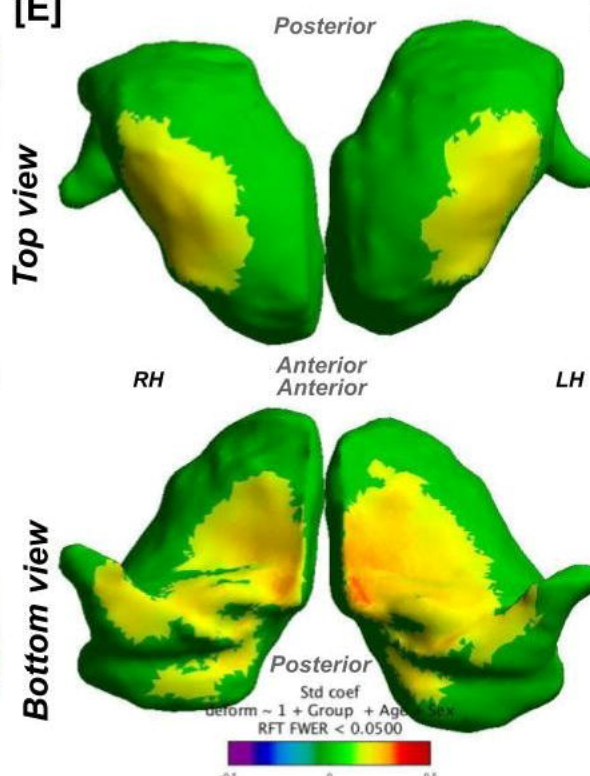
Thalamus

Pallidum

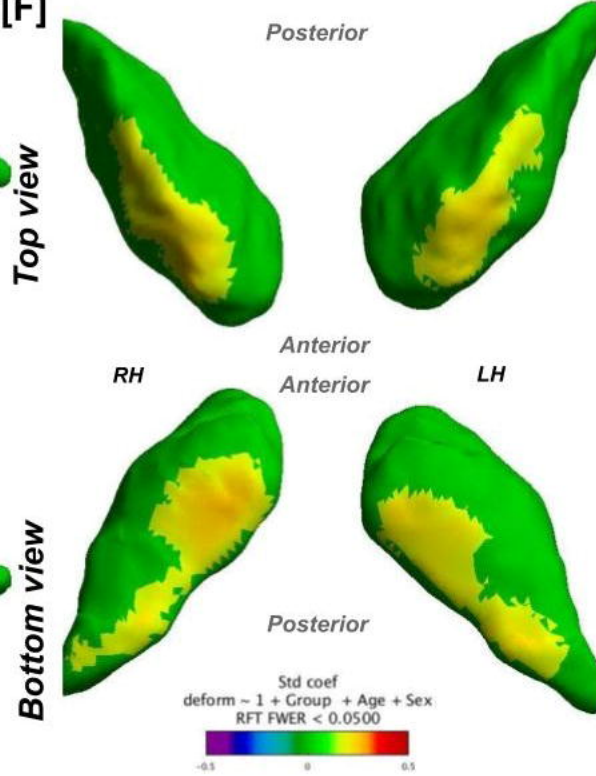
[D]



[E]



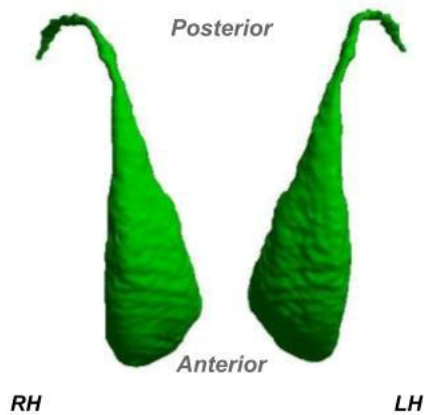
[F]



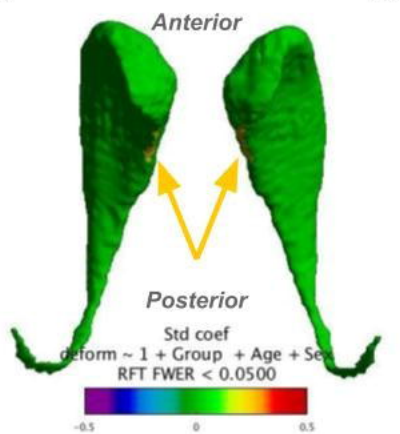
Caudate

[A]

Top view



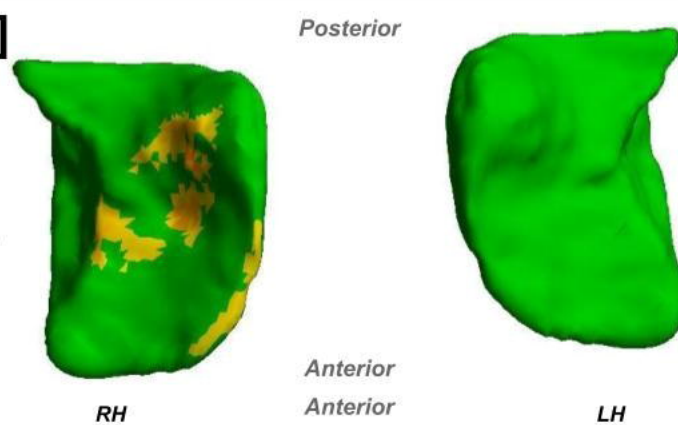
Bottom view



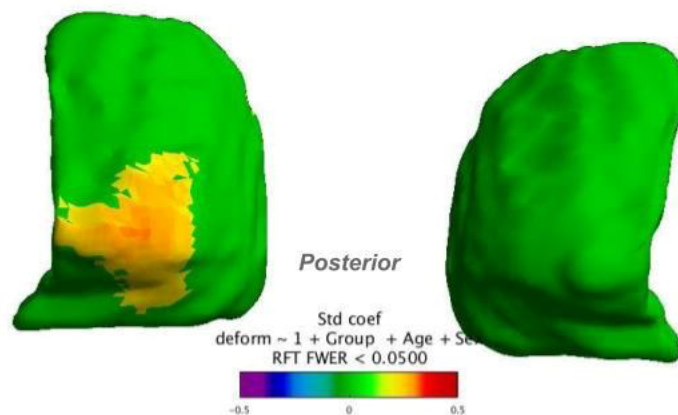
Accumbens

[B]

Top view



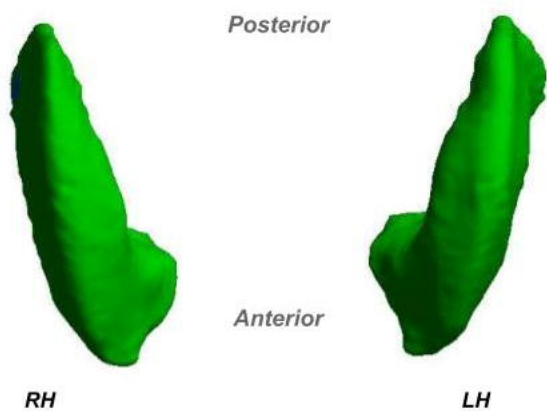
Bottom view



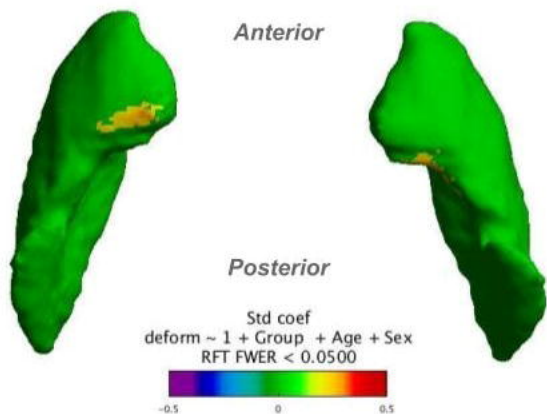
Putamen

[C]

Top view



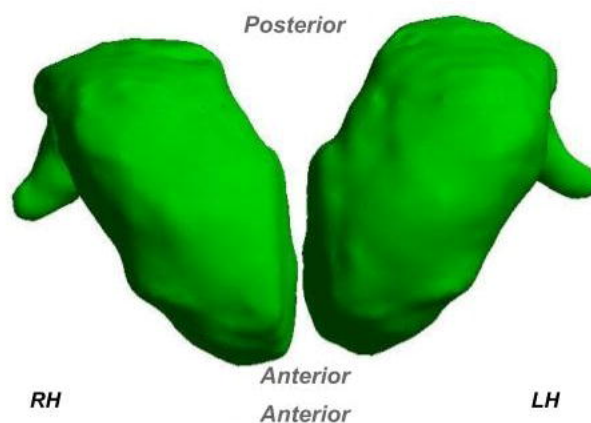
Bottom view



Thalamus

[D]

Top view



Bottom view

